جامعة عين شمس
Faculty of Women for, Arts, Science, and Education
Scientific Publishing Unit

Journal of Scientific Research in Science

Basic Sciences

Volume 40, Issue 1, 2023

ISSN 2356-8372 (Online) \ ISSN 2356-8364 (print)

Journal of Scientific Research in Science 2023, 40, (1): 1-14

Contents lists available at EKB

Journal of Scientific Research in Science

Journal homepage: https://jsrs.journals.ekb.eg/

Accurate Measurement of Surface Irregularities for a Standard Sphere Using Fizeau Laser Interferometer

Ahmed Ali[1, *], Mohamed Amer[1], Nadra Nada[2]

[1] Engineering and Surface Metrology Laboratory, National Institute of Standards (NIS), M. Anwar El-Sadat St., 12211 Giza, Egypt

[2] Physics Department, Faculty of Women for Arts, Science, and Education, Ain Shams University, Asmaa Fahmy St., 11757 Cairo, Egypt

Abstract:

Spherical surfaces are essential components in optical systems for different applications. Also, standard spheres are typically employed to calibrate dimensional and mass-measuring instruments. Therefore, measuring and eliminating the surface irregularities of these spheres represents a challenge for modern industries. Surface irregularities can be measured by either the contact method (as stylus profilometers) or the non-contact method (as interferometers). The Fizeau laser interferometer (GPI-XP, Zygo Co.) is typically used to accurately measure surface irregularities for flat surfaces, lenses, and mirrors of 102 mm diameter, and it is not prepared for testing heavy spheres. This work presents a modification for the interferometric system to expand its capability for testing spheres of diameters up to 145 mm and masses up to 2 kg. Also, the modification provides automatic rotation for the tested surfaces (an electric rotating platform) to avoid the disadvantages of manual rotation (a tweezer). At different rotation angles, the measurements are performed on a mass-standard silicon sphere (SiScKg-02-d, PTB Inst.). The average measured value of the surface irregularities is 43.9 nm, with an improved repeatability of 2.8 nm and a minimized measurement uncertainty of ±6.8 nm. The evaluation of the uncertainty budget is also investigated in this study.

Keywords: Fizeau, Interferometry, Surface irregularities, Silicon sphere.

***Corresponding author**: Ahmed Ali, Engineering and Surface Metrology Laboratory, National Institute of Standards (NIS), M. Anwar El-Sadat St., 12211 Giza, Egypt

E-mail: ahmed.ali@nis.sci.eg

(Received 03 July 2023, revised 18 July 2023, accepted 24 July 2023)

https://doi.org/10.21608/JSRS.2023.220756.1112

1. Introduction

Because of their excellent symmetry, high-quality spheres are frequently utilized for various applications, including bearings, optical surfaces, and volume definitions, as in the Avogadro project [1]. Furthermore, the precision spheres are considered calibration standards for dimensional measurement devices such as coordinate measuring machines (CMM) and surface profilometers [2]. Also, spherical optics are widely employed in several medical applications, from diagnostics to therapies to surgical operations [3]. In addition, large-radius mirrors and lenses are commonly employed in space applications and building detection imaging systems [4][5]. These high-quality spherical surfaces can be obtained by diverse techniques such as ultra-precision turning [6], high-speed polishing [7], centerless grinding of balls [8], and electrochemical polishing [9].

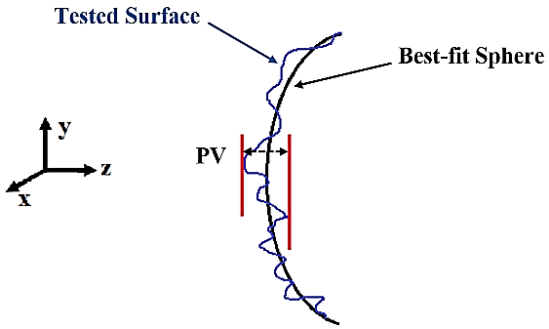

Fig. 1: PV-value, i.e., the distance from the highest point on the surface to the lowest one, scales the surface irregularities.

The surface irregularities depart from the best-fit sphere, represented by Peak-to-Valley (PV-value) [10]. PV-value is the distance from the highest point on the surface to the lowest one, as shown in **Fig. 1** [11]. Surface irregularities are a significant problem in characterizing the qualities of spherical surfaces; they appear as wrinkles, dents, plastic deformation, and warps [12]. Therefore, much valuable data is gained by measuring surface irregularities, such as wear resistance, sealing, friction, lubricant retention, contact ability, fatigue, performance of optical systems, and the accuracy of the radius of curvature [13][14] [15]. The surface irregularities can be measured by; *contact* and *non-contact* methods. Roundness measuring machines, coordinate measuring machines, and stylus profilometers belong to the contact techniques [16–18]. However, these techniques are fast but may harm high-quality surfaces [4]. Non-contact techniques include deflectometers, sub-aperture stitching interferometers, autocollimators phase-measuring interferometers, coherence scanning microscopes, confocal microscopes, optical profilers, and fringe projection profilometers [17–20]. However the high

resolution of these techniques, the accuracy is susceptible to the environment and the surface's reflectivity [17].

A Fizeau laser interferometer with a precise 5-axis mount is frequently employed to measure the surface irregularities of spherical surfaces, as shown in **Fig. 2a**. However, the manufacturers commonly support a non-rotatable mount with a self-centering clamp of 102 mm diameter, as shown in **Fig. 2b**; the challenge is testing high-quality spheres of larger diameters with automatic rotation. Some improvements were performed by previous works such as; mounting a convex lens of 260 mm diameter, but it not applicable for spheres and non-rotatable [21], a 3-pin mount to test a bulk sphere of 50 mm diameter, but it non-rotatable [22], a 3-pin mount to test a sphere of 93 mm diameter, but it non-rotatable [23], a rotating mount with vacuum chamber to test a sphere of 93 mm diameter, despite of high-accuracy, the high cost made this a problematic modification [24], a mount to test a sphere of 48 mm diameter, but it non-rotatable [25], a mechanically-rotating mount with spherical cavity has been developed to test a sphere of 93 mm diameter, but it needs an airtight vacuum, which makes it an expensive modification [26], a hollow mount made from Acrylic is employed to test a sphere of 93 mm diameter, but it non-rotatable [27], a mount to hold concave lens of 120 mm radius, but it not applicable for spheres and non-rotatable [28], a mount to test lenses and mirrors, with either concave or convex surfaces of diameters up to 1038 mm, this feature is not only applied for absolute wavelength tuning Fizeau interferometer but is also non-rotatable [29].

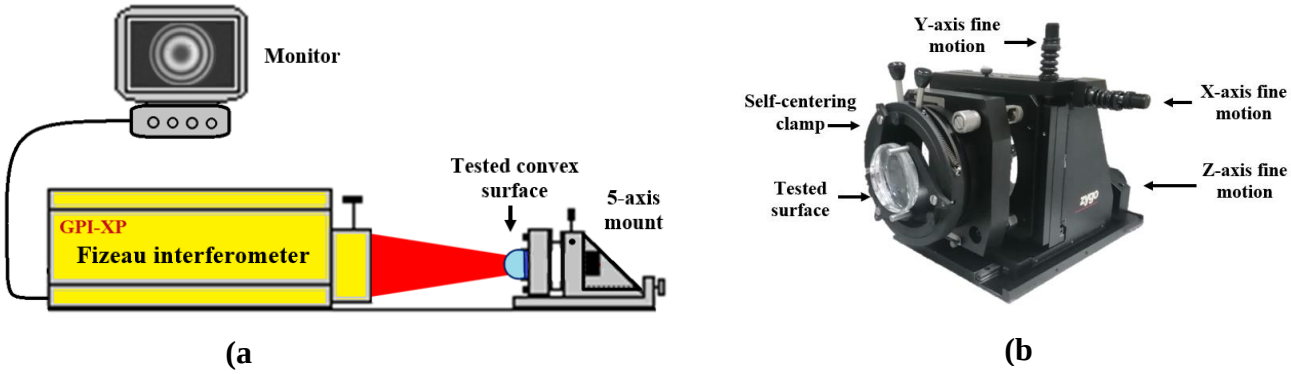

Fig. 2: (a) Fizeau laser interferometer with a 5-axis mount for testing a convex surface, (b) A default 5-axis mount gives a precise fine movement in +x, - x, +y, +z, and -z directions, with a self-centering clamp to hold tested spherical surfaces (usually are lenses or mirrors) with a maximum diameter of 102 mm.

This work offers a modification to a 5-axis mount of the Fizeau laser interferometer to expand its capability to test the high-quality spheres of diameters up to 145 mm and masses up to 2 kg. Also, an electric rotating platform (automatic rotation) is used to precisely swivel the

tested sphere at 360° around the y-axis, to avoid the errors caused by the manual rotation and improve the measurement repeatability. Furthermore, the evaluation of the uncertainty budget is included in this study.

2. Materials and Methods

2.1 Principle

Interferometers use the wave properties of light to analyze surface irregularities [30]. As shown in **Fig. 3**, a Fizeau interferometer with a laser head produces a beam of 632.8 nm wavelength; this beam is divided by a beam-splitter into two paths. The beam reflected off the reference surface (transmission sphere) is called the *reference* wavefront (W_r), and the beam reflected off the tested surface (silicon sphere) is called the *test* wavefront (W_t); these two beams are then reunited to represent a *measurement* wavefront (W_m) and directed to a CCD camera to analyze the resultant interferogram through appropriate software, as mentioned in **Eq. (1)** [10].

$$W_m = W_r + W_t \quad (1)$$

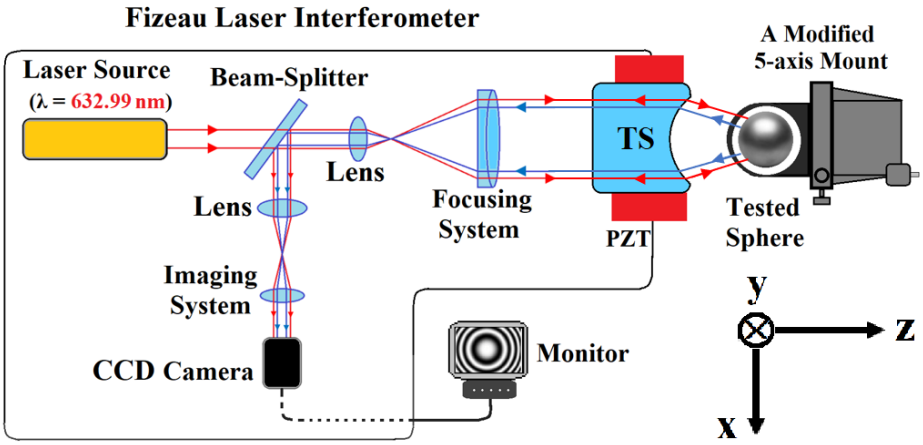

Fig. 3: Schematic diagram of phase-shifting Fizeau laser interferometer. A beam is emitted from a laser head, divided by a beam-splitter into two paths; the reference beam, which reflects off the transmission sphere (TS), and the test beam, which reflects off the tested sphere. The two beams are then recombined and captured by a CCD camera to analyze the interferogram.

The Fizeau interferometer has the advantage of phase shifting interferometry (PSI), a well-suited interferometric technique for testing spherical surfaces [31]. PSI relies on moving the reference surface forward and backward, generating consistent phase fluctuations between the reference wavefront (W_r) and the measurement wavefront (W_m), as expressed in **Eq. (2)** [32].

$$I_m = A + B + 2(AB)^{1/2} \cos [\varphi+\alpha] \quad (2)$$

Where (I_m) is the measured intensity, (A) is the background intensity function, (B) is the amplitude modulation function, (φ) is the phase difference of the interfering two wavefronts, and (α) is the phase shift of the m-th intensity measurement [32]. In order to solve the above non-linear equation, i.e., determination of (φ), at least (m ≥3) series of interferograms each of identical phase shift (α) must be captured. Piezoelectric transducers (PZT) are employed to precisely shift the reference surface; accordingly, (φ) is determined [32]. Hence, the obtained phase difference (φ) is converted to surface irregularities (PV-value) according to **Eq. (3)** [33].

$$PV\text{-value} = \frac{\varphi\lambda}{4\pi} \quad (3)$$

2.2. Experimental setup

A square-angle stainless-steel holder is installed to the 5-axis mount, as shown in **Fig. 4a**. A 360° electric rotating platform with 1° resolution (manufactured by RoHs, China) is adhered to the stainless-steel holder to support spheres of masses up to 2 Kg, as shown in **Fig. 4b**. The tested sphere is a mass or density standard sphere model made by PTB, Germany. It is a single silicon crystal, and its diameter is 93.6344 mm [34] [35].

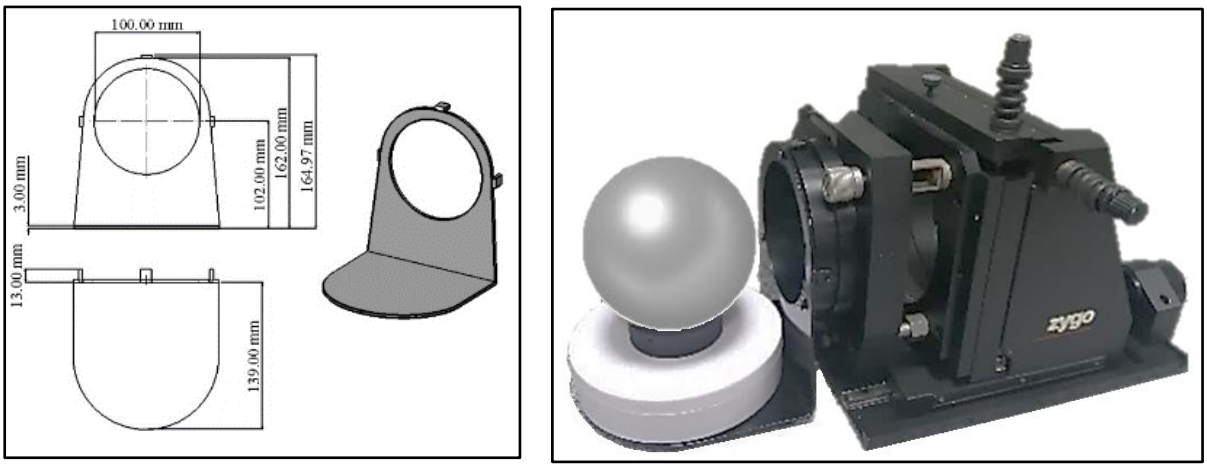

(a **(b**

Fig. 4: (a) Dimensions of the stainless-steel holder, (b) The modified 5-axis mount with the electric rotating platform and the tested silicon sphere.

Fig. 5 shows the experimental setup of the used system; a Fizeau laser interferometer (GPI-XP, Zygo) with a He-Ne beam (λ = 632.8 nm, diameter =102 mm). This system is supported by spherical reference surfaces called transmission spheres (TS), selected from the *f*/0.65 to *f*/11 range, and offers enough versatility for testing both convex and concave spherical surfaces [36]. For *f*/number or (*f*/#), the word "number" refers to the ratio of the TS's focal length to the TS's entrance pupil diameter [36]. A 5-axis mount gives a fine movement in +x, - x, +y, +z, and -z directions to accurately align the tested surface with the axis of the reference surface. The *MetroPro 7.3.2* software operates this system. It is crucial to measure the environmental conditions to calculate the air-refractive index accurately. Thermocouples module NI 9211 is used for measuring the temperature, manufactured by National Instruments, Texas, USA. Atmospheric pressure is monitored by a TM-414 digital barometer manufactured by Tenmars, Taiwan. Data logger 175H1 is used for measuring relative humidity, manufactured by Testo, Germany. Also, a VB-8200 vibration meter is manufactured by Lutron Electronics, USA. The system is built on a vibration isolation table manufactured by Melles Griot, USA.

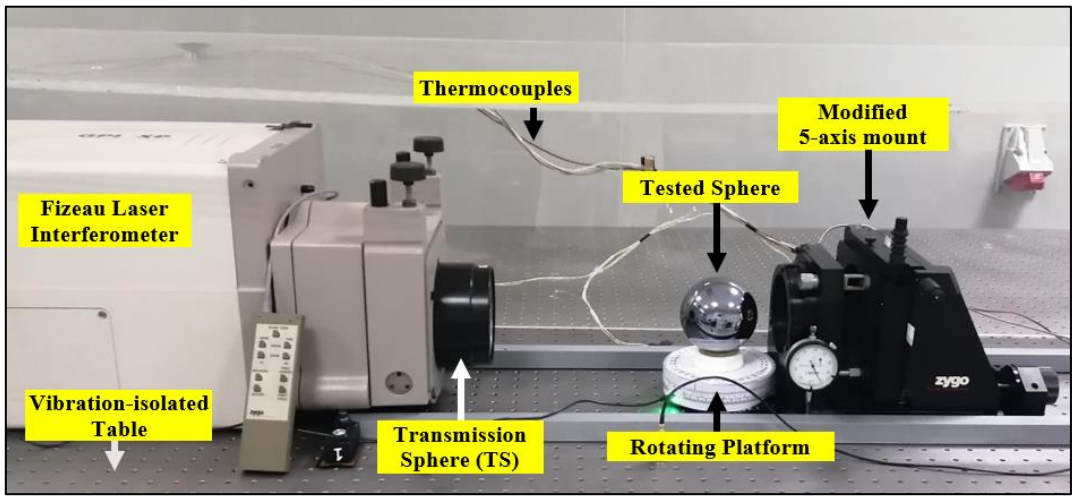

Fig. 5: Experimental setup of the Fizeau laser interferometer with the modified 5-axis mount. The above system is employed for measuring the surface irregularities of a silicon sphere of 93 mm diameter.

2.3. Measurement of surface irregularities

MetroPro 7.3.2 software is used for measuring the absolute surface irregularities for both reference and tested surfaces by subtracting the wavefront data of the tested surface from the acquired wavefront data [37]. The measurement is divided into two main steps; the first step is locating the tested surface at the confocal position, i.e., when the focal point of the transmission sphere coincides with the center of curvature of the tested sphere, as shown in

Fig. 6a. The confocal position is detected by the monitor when the concentric circular fringes are appeared, as shown in **Fig. 6b**. Second step is capturing the interference fringes at different rotations.

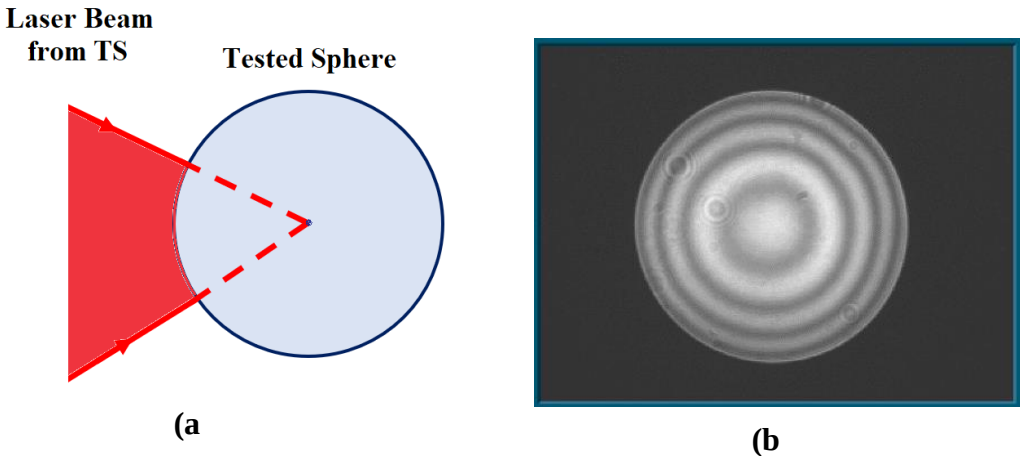

Fig. 6: (a) Schematic diagram of the confocal position; the laser cone focus coincides with the center of curvature of the tested sphere, (b) The fringes of the confocal position appeared at the monitor.

3. Results and Discussion

The testable area is dependent on the TS used; the smaller the *f/number* TS, the wider the tested area, provided that $r \leq f$, where (r) is the radius of curvature of the tested surface and (f) is the focal length of the transmission sphere. **Fig. 7** shows 3-D maps for 2 cm^2 of the tested surface obtained by the *f*/3.3 transmission sphere. The shown measurements are the peaks and valleys in wave units; they can be converted to *nm* by multiplying with λ (λ= 632.8 nm). The measurements are conducted by the automatic rotation and taken in different rotations, typically at 0°, 90°, 180° and 270°.

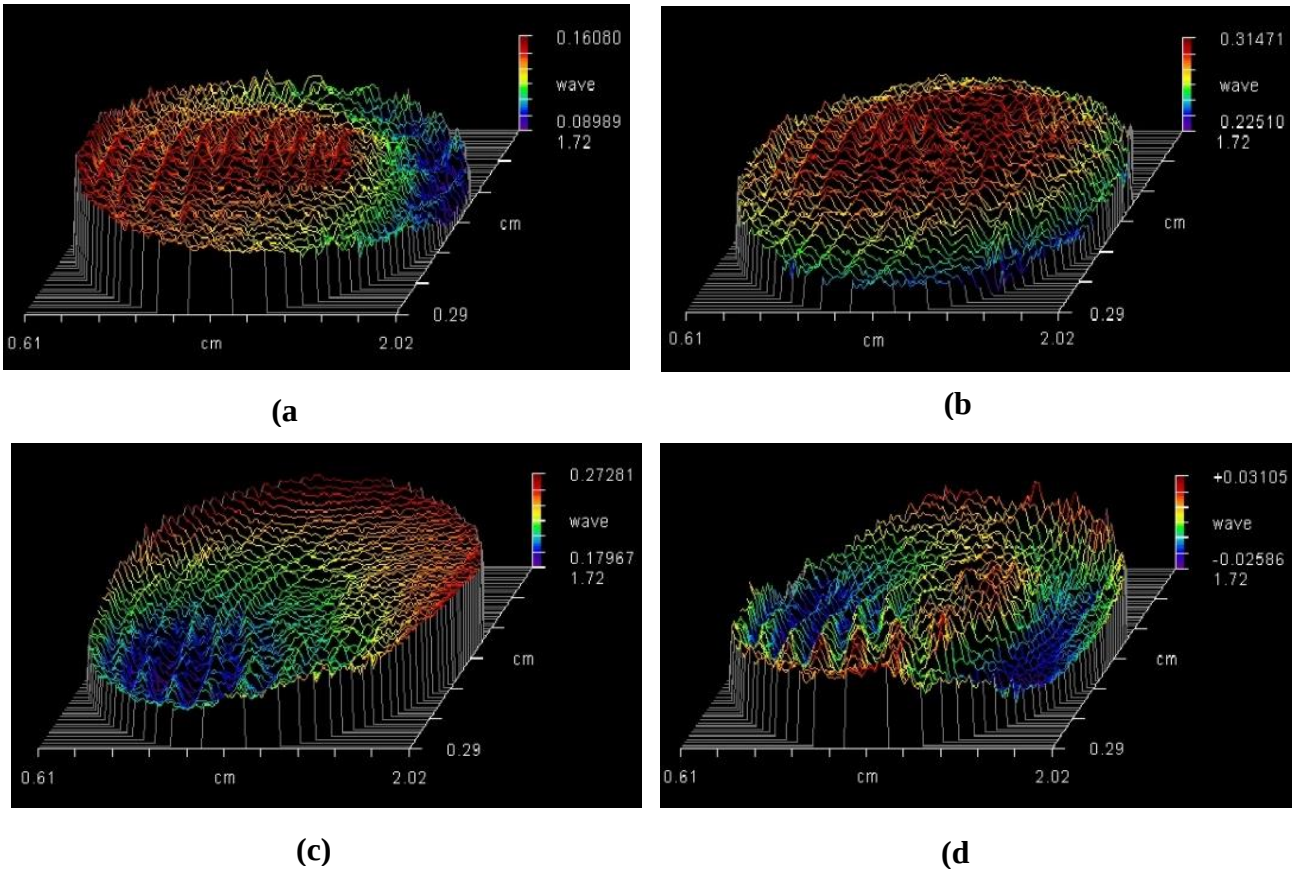

Fig. 7: The measured surface irregularities are represented by 3D maps of the tested surface; (a) at 0° rotation angle, (b) at 90° rotation angle, (c) at 180° rotation angle, (d) at 270° rotation angle.

The manual rotation is typically accompanied by measurement errors, such as transferring heat from the user's hand to the tweezer to the tested surface, leading to temperature inhomogeneity. Also, the misalignment caused by the emerged vibration due to the manual rotation of the tested surface and potential damage to high-quality surfaces due to pressure from the tweezer. Also, the tweezer's liner may leave residual tissues or dust on the measured surface, resulting in false measurement results. Also, incorrect data entry, as the *MetroPro* software relies on a series of measurements with distinct rotation angles, the tolerance in the rotation angle causes an arithmetic error within the program, thus reducing confidence in the presented results. All the previous errors are eliminated when using the automatic rotation, consequently improving the repeatability of results. **Fig. 8** shows the measured surface irregularities (PV-values) using manual and automatic rotation. Five measurements are conducted in the same position corresponding to the same rotation angle. Each measurement is indicated by an *error bar* equivalent to the standard deviation of the five results; it is clear that the automatic rotation is more accurate because it represents a shorter error bar.

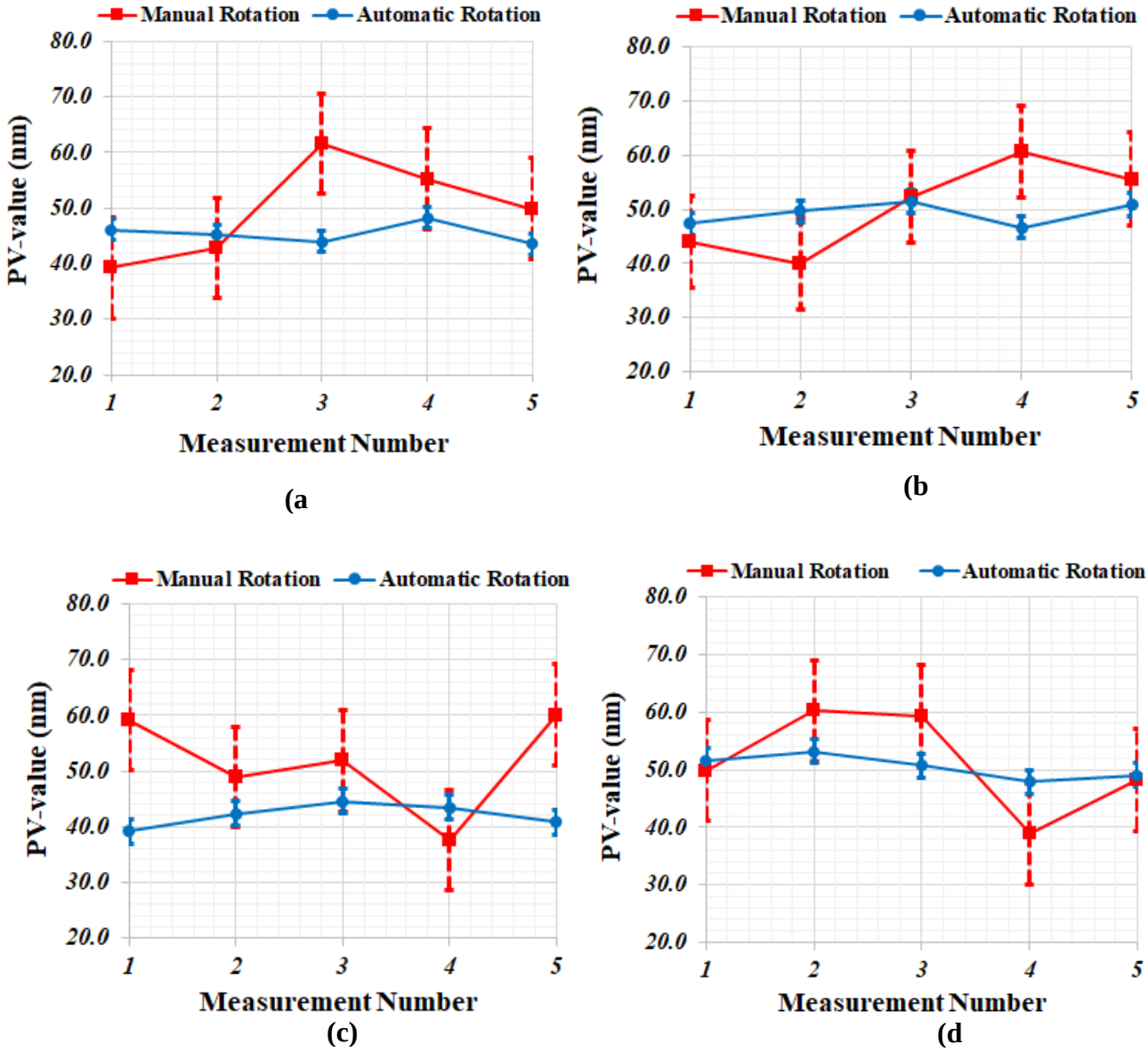

Fig. 8: The measured surface irregularities for a portion of the silicon sphere using manual and automatic rotation. Each curve represents five measurements in the same position, i.e., the same rotation angle. Each measurement is indicated by an *error bar* equivalent to the five measurements' standard deviation. (a) At 0° rotation angle, (b) at 90° rotation angle, (c) at 180° rotation angle, (d) at 270° rotation angle.

The average measured PV-value for ten points in horizontal and vertical directions along the diameter of the tested sphere, as shown in **Fig. 9**. The manual rotation introduced a 51.8 nm for the measured surface irregularities with a standard deviation of 13.0 nm. The standard deviation contributes mainly to the measurement uncertainty, so the measurement uncertainty, in this case, is ±15.5 nm. When using the automatic rotation, the value of the measured surface irregularities is 43.9 nm with a reduced standard deviation of 2.8 nm, leading

to minimizing the measurement uncertainty to ±6.8 nm, as shown in **Fig. 9.** Each measurement is indicated by an *uncertainty bar*, the shorter this bar is, the higher the degree of confidence in the measured results.

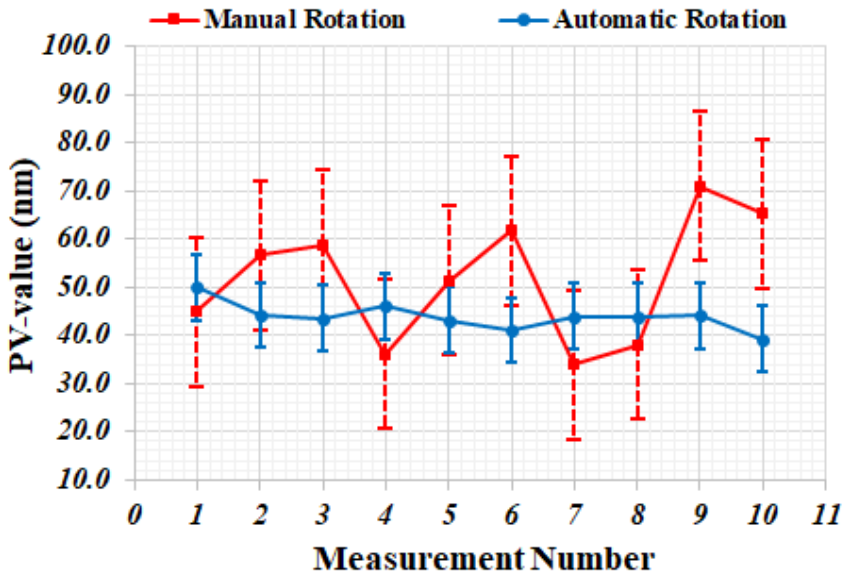

Fig. 9: The average measured surface irregularities for ten points located in horizontal and vertical directions along the diameter of the tested sphere, each measurement associated with an uncertainty bar. The manual rotation represents a measured PV-value of 51.8±15.5 nm, but the automatic rotation represents a measured PV-value of 43.9±6.8 nm.

The degree of confidence in the measured values is scaled with the expanded measurement uncertainty, which depends on factors such as the used wavelength, environmental conditions, and reference optics. For example, the wavelength is calibrated against the *Optical Spectrum Analyzer* and is found to be 632.99±0.02 nm. Thus, the used system is traceable to the International System of Units (SI unit) through the primary length standard at the National Institute of Standards (NIS), Egypt. Also, the environmental conditions are monitored, and the limits of the reference optics are stated by the manufacturer. The main factors that contribute to the measurement uncertainty are investigated according to the *Guide to the Expression of Uncertainty in Measurement* (GUM) [38], as listed in **Table (1).**

Symbol	Source of Uncertainty	Limits	Unit	Type	Distribution	Dividor	Sensitivity coefficient (C_i)	Uncertainty contribution, u_i (nm) (Limits×Dividor×C_i)
u_1	Repeatability	2.8	nm	A	N	$1/\sqrt{4}$	1	1.4
u_2	Wavelength Stability	0.02	nm	B	N	1/2	1	0.01
u_3	Temperature	0.11	°C	B	R	$1/\sqrt{3}$	-9.50×10^{-7}	-6.03×10^{-8}
u_4	Air pressure	24.20	Pa	B	R	$1/\sqrt{3}$	2.67×10^{-6}	3.74×10^{-5}
u_5	Humidity	0.69	%RH	B	R	$1/\sqrt{3}$	-8.82×10^{-9}	-3.52×10^{-9}
u_6	TS Wavefront Errors	5.00	nm	B	R	$1/\sqrt{3}$	1	2.9
u_7	Air Turbulences	2.00	nm	B	N	1/2	1	1.0
u_8	Rotaion Angle	1.00	degree	B	R	$1/\sqrt{3}$	1	0.5
Expanded Uncertainty (k=2) =							$(\sqrt{u_1^2+u_2^2+u_3^2+u_4^2+u_5^2+u_6^2+u_7^2+u_8^2})\times k$	± 6.8 nm

Table (1): The calculations of the measurement uncertainty according to GUM [38].

4. Conclusion

Measuring the surface irregularities of a standard sphere is of industrial and metrological importance. When a Fizeau laser interferometer (GPI-XP, Zygo Co.) with a 5-axis mount is used to conduct these measurements, two problems must be solved. The first problem is the system's inability to accommodate bulky or heavy spheres because the 5-axis mount is supported by a self-centering clamp to hold only flat surfaces, lenses, and mirrors of diameters up to 102 mm. The second problem is that the manual rotation (tweezer) yields poor measurement accuracy and exposes the tested surface to damage. Therefore, a modification is performed on the 5-axis mount by installing a stainless-steel holder and an electric rotating platform (E10336W, RoHs Co.). Thus, the capability of the interferometric system is expanded to test spheres of diameters up to 145 mm and masses up to 2 Kg with a precise automatic rotation. The tested surface dealt with in this study is a mass standard silicon sphere (SiScKg-02-d, PTB Inst.) of 93.6 mm in diameter and 1 Kg in mass. The measurements are conducted at four rotation angles 0°, 90°, 180° and 270° through manual and automatic rotation. The repeatability of results is improved because the automatic rotation yielded an average measured value for the surface irregularities of 49.3 nm with a standard deviation of 2.8 nm, whereas the manual rotation yielded an average measured value of 51.8 nm with a standard deviation of 13.0 nm. Furthermore, the measurement accuracy is enhanced because the automatic rotation presented a minimized measurement uncertainty of ±6.8 nm, while the manual rotation yielded a large measurement uncertainty of ±15.5 nm. The traceability of the used laser system is achieved through a He-Ne laser head of 632.8 nm in wavelength. Also, the evaluation of the uncertainty budget is included in this work. Future research may address the improvement of the system to test larger standard spheres with diameters longer than 145 mm.

Acknowledgments The authors are grateful for Eng. Hussein Zayed (NIS, Egypt) for his technical support.

Conflict of interest The authors have no competing interests to declare that are relevant to the content of this article.

References

[1] R.B. Eisswanger, M.W. Eckerle, C.P. Russ, S.R. Eichelt, Interferometric Radius of Curvature Measurements : An Environmental Error Treatment, Opt. Express 30: (2022) 25803–25816.
[2] K. Liu, Y. Liang, M. Tang, Calibration Method for Structural Parameters of the Articulated Arm Coordinate Measuring Machine Utilizing a Modified Hybrid Algorithm, Meas. Sci. Technol. 34: (2023) 1–19.
[3] M.D. Al-amri, M.M. El-gomati, M.S. Zubairy, Optics in Our Time, Springer, (2016), King Abdulaziz City for Science and Technology.
[4] W. Gong, J. Dou, Y. Hu, Z. Yang, Fast Measurement Strategy for Large Radius of Curvature, Opt. Laser Technol. 161: (2023) 1–8.
[5] Y. Zhong, J. Chang, X. Zhao, S. Du, Y. Mu, H. Jiang, X. Li, Optical Design and Implementation of a Compact and Long Focal Length Imaging System, Opt. Lasers Eng. 163: (2023) 1–7.
[6] D. Li, X. Jiang, Z. Tong, L. Blunt, Kinematics Error Compensation for a Surface Measurement Probe on an Ultra-Precision Turning Machine, Micromachines 9: (2018) 1–15.
[7] H. Zhang, P. Wang, Z. Li, Y. Shen, X. Zhang, Uniform Polishing Method of Spherical Lens Based on Material Removal Model of High-Speed Polishing Procedure, Micromachines 11: (2020) 1–14.
[8] O.P. Reshetnikova, B.M. Iznairov, A.N. Vasin, N. V. Belousova, A. V. Panfilova, Correction of Form Errors during Centerless Grinding of Balls, J. Phys. Conf. Ser. 1515: (2020) 1–7.
[9] U.S. Kim, J.W. Park, High-Quality Surface Finishing of Industrial Three-Dimensional Metal Additive Manufacturing Using Electrochemical Polishing, Int. J. Precis. Eng. Manuf. - Green Technol. 6: (2019) 11–21.
[10] U. Griesmann, Q. Wang, J. Soons, R. Carakos, A Simple Ball Averager for Reference Sphere Calibrations, SPIE 5869: (2005) 1–8.
[11] ISO, Geometrical product specifications ISO 25178-2:2012, ISO, (2012), Geneva.
[12] K. Kase, A. Makinouchi, T. Nakagawa, H. Suzuki, F. Kimura, Shape Error Evaluation Method of Free-Form Surfaces, CAD Comput. Aided Des. 31: (1999) 495–505.
[13] Y. Guo, A Surface Shape Test Method for a Thin Flat Mirror, Optik (Stuttg). 152: (2018) 116–126.
[14] P. Podulka, Selection of Methods of Surface Texture Characterisation for Reduction of the Frequency-Based Errors in the Measurement and Data Analysis Processes, Sensors 22: (2022) 1–23.
[15] A. Ali, M. Amer, N. Nada, Error Analysis of Laser Interferometric System for Measuring Radius of Curvature, J. Opt. (2023) 1–14. https://doi.org/10.1007/s12596-023-01269-9
[16] R. Thalmann, Basics of Highest Accuracy Roundness Measurement, Simp. Metrol. 25: (2006) 1–6.
[17] Y. Shen, J. Ren, N. Huang, Y. Zhang, X. Zhang, L. Zhu, Surface Form Inspection with

Contact Coordinate Measurement: A Review, Int. J. Extrem. Manuf. 5: (2023) 1–29.
[18] J. Spichtinger, M. Schulz, G. Ehret, R. Tutsch, Traceable Stitching Interferometry for Form Measurement of Moderately Curved Freeform Surfaces, Opt. Eng. 61: (2022) 1–18.
[19] J. Béguelin, T. Scharf, W. Noell, R. Voelkel, Correction of Spherical Surface Measurements by Confocal Microscopy, Meas. Sci. Technol. 31: (2020).
[20] G. Udupa, B.K.A. Ngoi, Form Error Characterisation by an Optical Profiler, Int. J. Adv. Manuf. Technol. 17: (2001) 114–124.
[21] J.H. Burge, Fizeau Interferometry for Large Convex Surfaces, SPIE 2536: (1995) 127–138.
[22] T.L. Schmitz, C.J. Evans, A. Davies, W.T. Estlerl, Displacement Uncertainty in Lnterferometric Radius Measurements, CIRP Ann. 51: (2002) 1–4.
[23] U. Griesmann, J. Soons, Q. Wang, Measuring Form and Radius of Spheres with Interferometry, CIRP Ann. 53: (2004) 451–452.
[24] R.A. Nicolaus, C. Elster, Diameter Determination of Avogadro Spheres #1 and #2, IEEE Trans. Instrum. Meas. 54: (2005) 872–876.
[25] T.L. Schmitz, N. Gardner, M. Vaughn, K. Medicus, A. Davies, Improving Optical Bench Radius Measurements Using Stage Error Motion Data, Appl. Opt. 47: (2008) 6692–6700.
[26] Z. Luo, Y. Gu, J. Zhang, L. Yang, L. Guo, Interferometric Measurement of the Diameter of a Silicon Sphere With a Mechanical Scanning Method, 59: (2010) 2991–2996.
[27] X. Wu, Y. Li, H. Wei, H. Yang, G. Yang, Interferometric Diameter Determination of a Silicon Sphere Using a Traceable Single Laser Frequency Synthesizer, Meas. Sci. Technol. 24: (2013) 1–9.
[28] M. Jie, H. Xi, W. Fan, The Effects of Thermal Field on Radius of Curvature Interferometric Testing, Opt. Rev. 22: (2015) 299–307.
[29] J. Kredba, P. Psota, M. Stašík, V. Lédl, L. Veselý, J. Nečásek, Absolute Interferometry for Fast and Precise Radius Measurement, Opt. Express 29: (2021) 12531–12542.
[30] Zygo Corporation, Phase Shifting Interferometry, (2014), Middlefield, USA.
[31] D. MALACARA, Optical Shop Testing, John Wiley & Sons, (2007), New Jersey.
[32] G. Moona, R. Sharma, U. Kiran, K.P. Chaudhary, Evaluation of Measurement Uncertainty for Absolute Flatness Measurement by Using Fizeau Interferometer with Phase-Shifting Capability, Mapan - J. Metrol. Soc. India 29: (2014) 261–267.
[33] K. Creath, Step Height Measurement Using Two-Wavelength Phase-Shifting Interferometry, Appl. Opt. 26: (1987) 2810–2816.
[34] T. Schmiermund, The Measurement of the Avogadro Constant, Springer, (2022), Frankfurt am Main, Germany.
[35] H. Bettin, K. Fujii, A. Nicolaus, Silicon Spheres for the Future Realization of the Kilogram and the Mole, Comptes Rendus Phys. 20: (2019) 64–76.
[36] Zygo Corporation, Transmission Sphere Selection SB-0297, Zygo Corporation, (2014), Middlefield, USA.
[37] Zygo Corporation, Two Sphere - MetroPro Application OMP-0388B, Zygo Corporation, (2004), Middlefield, USA.
[38] BIPM, IEC, IFCC, ILAC, ISO, IUPAC, IUPAP, OIML, Guide to the expression of uncertainty in measurement (JCGM 100:2008), BIPM, (2004), Saint-Cloud.

الملخص العربى

قياس دقيق لأخطاء السطح لكرة عيارية بإستخدام مقياس التداخل الليزري" فيزو"

أحمـد علـي[1،*] ، محمـد عامــر[1] ، نــادرة نــدا[2]

1- معمل المترولوجيا الهندسية والسطوح، المعهد القومي للمعايرة، شارع الزعيم محمد أنور السادات، الرمز البريدي: 12211 الجيزة، مصر.

2- قسم الفيزياء، كلية البنات للآداب والعلوم والتربية، جامعة عين شمس، شارع أسماء فهمي، الرمز البريدي: 11757 القاهرة، مصر.

(*المؤلف المراسل: ahmed.ali@nis.sci.eg)

الملخص باللغة العربية

يُعدَ قياس الأخطاء السطحية لكرة عيارية ذا أهمية صناعية ومترولوجية. هناك مشكلتين يجب حلّهما عند استخدام مقياس التداخل بالليزر Fizeau (GPI-XP, Zygo Co.)، والمزوّد بحامل خماسي المحاور لإجراء هذه القياسات. المشكلة الأولى هي عدم قدرة النظام على استيعاب الكرات الضخمة أو الثقيلة لأن الحامل خماسي المحاور مدعوم بماسك ذاتي التمركز لحمل الأسطح المستوية والعدسات والمرايا بأقطار تصل إلى 102 مم. المشكلة الثانية هي أن الدوران اليدوي (الملقط) ينتج عنه دقة قياس ضعيفة ويعرض السطح المختبر للتلف. لذلك تم إجراء تعديل على الحامل خماسي المحاور عن طريق تثبيت حامل من الفولاذ المقاوم للصدأ ومنصة دوارة كهربائية (E10336W, RoHs Co.) ، وبالتالي تم زيادة قدرة النظام لاختبار الكرات المصمتة والثقيلة بأقطار تصل إلى 145 مم وكتل تصل إلى 2 كجم مع دوران أوتوماتيكي دقيق. السطح الذي أُجريت عليه القياسات في هذا العمل هو كرة سيليكون قياسية الكتلة (SiScKg-02-d, PTB Inst.) ، بقطر 93.6344 مم وكتلة 1 كجم. تم إجراء القياسات بأربع زوايا دوران 0 درجة و 90 درجة و 180 درجة و 270 درجة من خلال الدوران اليدوي والتلقائي. وبناءا على ذلك تم تحسين تكرارية النتائج ،حيث أن الدوران التلقائي للسطح المقاس أسفر عن متوسط قيمة مقاسة لأخطاء السطح تبلغ 49.3 نانومتر مع إنحراف معياري قدره 2.8 نانومتر في حين أن الدوران اليدوي أسفر عن متوسط قيمة مقاسة 51.8 نانومتر مع إنحراف معياري قدره 13.0 نانومتر. علاوة على ذلك تم تحسين دقة القياس،حيث أن الدوران التلقائي للسطح المقاس أظهر قيمة مصغرة لعدم اليقين في القياس بقيمة ±6.8نانومتر، في حين أن الدوران اليدوي أسفر عن قيمة كبيرة لعدم اليقين في القياس وتبلغ ±15.5 نانومتر. تم تحقيق الإسناد المترولوجي للنظام المستخدم من خلال مصدر ليزر (He-Ne) ذات طول موجي 632.8 نانومتر. أيضا تم تضمين تقييم ميزانية اللايقين للقياسات في هذا العمل. قد تتناول الأبحاث المستقبلية تحسين النظام لاختبار كرات قياسية أكبر بأقطار أطول من 145 مم.